www.czasopisma.pan.pl PAN POLSKA AKADEMIA NAUK www.journals.pan.pl

Arch. Metall. Mater. **64** (2019), 3, 835-839

DOI: 10.24425/amm.2019.129457

SU-WON YANG*, JEONG-GON KIM*#, KWANG-PIL JEONG*,
HAN-UL SHIM*, SEONG-IL CHO*, MIN-YOUNG KIM*

CHANGE OF EASY MAGNETIZATION AXIS AND FREQUENCY OF REFLECTION LOSS BY Co-Ti SUBSTITUTION IN BARIUM FERRITE

In this study, $BaFe_{12-2x}Co_xTi_xO_{19}$ (X : 0 to 2.0, 0.2) powders were synthesized by sol-gel process. TG-DTA, XRD, SEM, VSM, and Network analyzer were measured in order to influence easy magnetization axis change on the wave absorption frequency range change. The easy magnetization axis change of the annealed powder at 900°C and 1200°C was confirmed by the coercive force decreased 4,800 and 3,870 Oe to 260 and 269 Oe, respectively, at the substitution ratio of 0.8 and 1.0. And it was confirmed that the change of the easy magnetization axis affected the change of the wave absorption frequency. The wave absorption frequency of substituted Barium Ferrite was less than 10 GHz range after the easy magnetization axis of Barium ferrite changed to a-b plan direction. It was confirmed the $BaFe_{12-2x}Co_xTi_xO_{19}$ (x = 0.8 to 1.6) was synthesized by the sol-gel process and it was annealed at 900°C and 1200°C, which could be used as a wave absorber in the X-band region of 10 GHz less.

Keywords: Barium ferrite, Co-Ti substitution, Easy magnetization axis

1. Introduction

Barium Ferrite (BaM, $BaFe_{12}O_{19}$) was a magnetoplumbite structure. Its structure was composed of a stacking layer of RSR* along the c-direction [1]. Thus, it showed an easy magnetization axis fixed strongly in the c-direction and the magnetic anisotropy with the c-direction [2]. Because of structural characteristic, the Barium ferrite revealed the hard magnetic property. When the barium ferrite was used as a wave absorber, it showed the wave absorption range of K band of 47.6 GHz [3]. The wave absorption property caused by the magnetic properties of barium ferrite, the change of magnetic properties of the barium ferrite influenced the change of the wave absorption range of the barium ferrite [4]. Therefore, the change of magnetic properties and the wave absorption range were confirmed by the effect of the substitutional ion pair in the barium ferrite. The substitutional ion pair was composed of divalent ion and tetravalent ion to maintain the overall electrical neutrality.

In our last study, as a result of the substitution of the pair of ions such as Co-Ti, Cu-Ti, Ni-Ti, and Mn-Ti, the substitution of the Co-Ti ion pair had the greatest influenced to the magnetic properties of barium ferrite. In this study, the change of magnetic properties of BaM and the easy magnetization axis of BaM with substitution ratio of Co^{2+} and Ti^{4+} ion pair were analyzed. It confirmed that availability of BaM as an X-band range wave absorber.

2. Experimental

$BaFe_{12-2x}Co_xTi_xO_{19}$ (X : 0~2.0, 0.2) powders were prepared by sol-gel process. Iron nitrate ($Fe(NO_3)_3 \cdot 9H_2O$), Barium nitrate ($Ba(NO_3)_2$), Cobalt acetate ($Co(CH_3COO)_2$), and Titanium isopropoxide ($Ti[OCH(CH_3)_2]_4$) were used as starting materials. They were mixed by stoichiometric ratio and were dissolved in deionized water (D.I). The citric acid and the ethylene glycol were added to the mixture. Then, the acidity of the mixture was adjusted to pH 6 by an ammonia solution. The mixture was heated and refluxed at 85°C for 15hours until it became a sol. The sol was heated and stirred to 98°C until it was transformed to gel on a hot plate. The gel was annealed in the atmosphere at 900°C and 1200°C for 3 hours, and then it was cooled down to room temperature in a furnace. The Barium Ferrite crystal forming process was confirmed by TG-DTA analysis (PerkinElmer STA8000). The crystal structure of the powder of BaM and substituted BaM were analyzed by XRD (Rigaku, smartLab, Cu Kα, $\lambda = 0.15425$ nm). Particle size and shape of BaM and substituted BaM were investigated by FE-SEM (JEOL, JSM-7800F). Saturation magnetization (M_s), and Coercive force (H_c) were measured by VSM (Quantum Design, VersaLab VSM). Reflection loss was measured by a Network Analyzer (Agilent PNA-X, airline). The sample of reflection loss was prepared as the toroidal type with outer diameter 7 mm, inner diameter 3.04 mm, and thickness 1 mm. The mixing ratio

* MATERIAL SCIENCE & ENGINEERING, INCHEON NATIONAL UNIVERSITY, 119 ACADEMY-RO, YEONSU-GU, INCHEON, 22012, KOREA
# Corresponding author: jyj309@inu.ac.kr

of powder and wax was 1.5:1. μ', μ'', ε', and ε'' were measured by network analyzer, and reflection loss was calculated by equation (1)

$$\text{Reflection loss (dB)} = -20\log_{10}|\Gamma| \quad (1)$$

$$\Gamma = \frac{Z_L - Z_S}{Z_L + Z_S}$$

3. Results and discussion

TG-DTA results are displayed in Fig. 1. From TG-DTA result, it could be confirmed that weight reducing in the annealing process and crystal generation and change. The weight reducing and the endothermal reaction at the 200°C could be confirmed. That was caused by the burnout process of the residue of the sol-gel process. The endothermic reaction at 200°C to 350°C was confirmed to be due to the nucleation reaction of BaM and substituted BaM crystal. The subsequent exothermic reaction was confirmed to be a crystal growth and the oxidation reaction. In the above 900°C, it was confirmed the crystal growth occurred continuously. This means that the crystal formation of BaM was completed before 900°C. Thus, we set the annealing temperature at 900°C and 1200°C in order to confirm the change of magnetic property by crystal size.

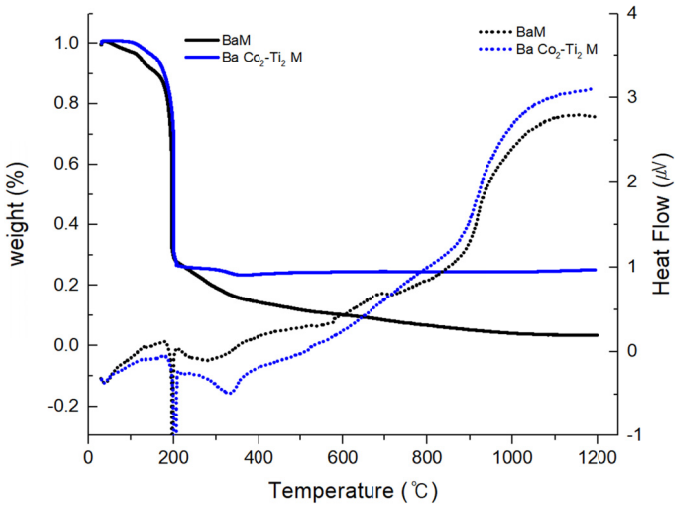

Fig. 1. TG-DTA result. Weight change and Heal flow of BaM and $BaCo_2Ti_2M$

XRD analysis was performed to confirm the lattice structure, crystallinity, and lattice size of the annealing samples. The XRD pattern of BaM and substituted BaM are displayed in Fig. 2. It can be seen that peaks of all compositions were located to the same degree. It means that all compositions have the same lattice structure, magnetoplumbite structure. It could confirm that sol-gel process and annealing process were suitable to make magnetoplumbite structure. The lattice parameter and FWHM(Full Width at Half Maximum) were analyzed to confirm the effect of substitution ion and annealing condition on the structure. These are displayed in Fig. 3. In the Fig. 3a), lattice parameter of a and c direction is displayed. The a-direction lattice parameter has shown the change of 5.892 to 5.897 Å, and c-direction lattice parameter has done 23.215 to 23.275 Å. This result caused by difference radius of Fe ion and substitution ions, Fe^{3+}, 72.5 pm, Co^{2+}, 88.5 pm, and Ti^{4+}, 74.5 pm, respectively. In addition, the substitution ions were mainly substituted in site along the c-direction on magnetoplumbite structure [5]. Therefore, the c-direction lattice parameter was increased with substitution ratio increasing.

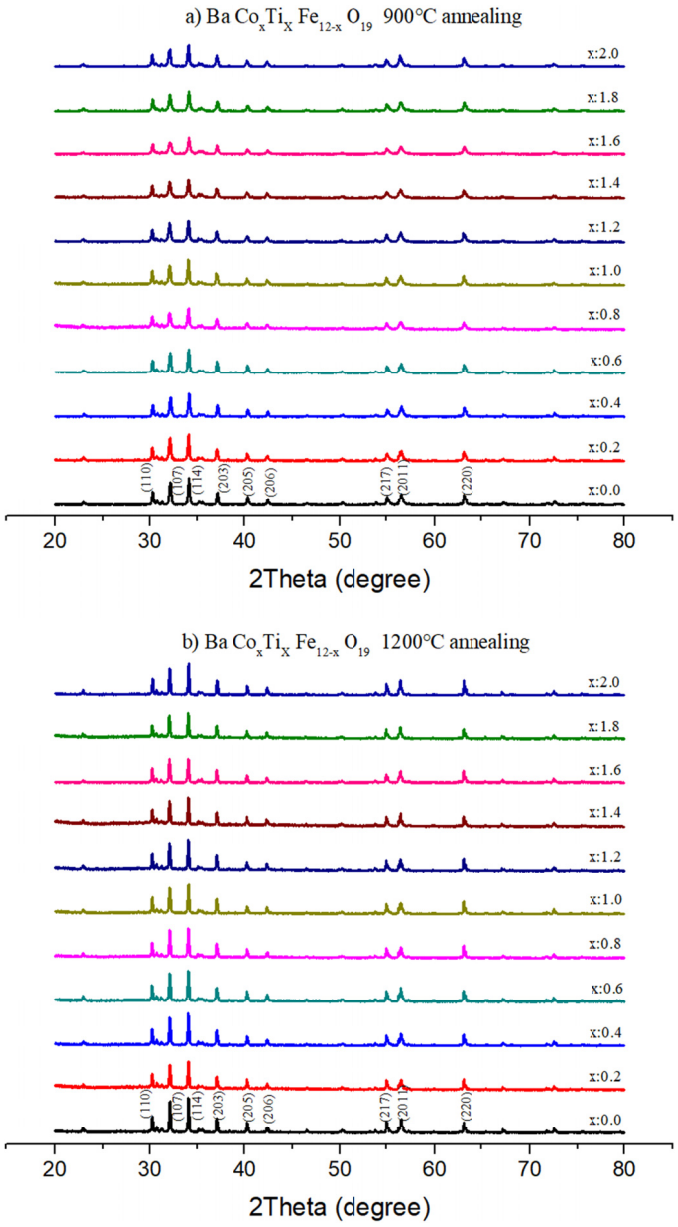

Fig. 2. XRD pattern of annealed BaM and substituted BaM, annealing temperature of a) 900°C and b) 1200°C

The FWHM of the BaM and substituted BaM was analyzed to confirm the crystallinity and crystal size. The FWHM of BaM and substituted BaM is displayed in the Fig. 3a). The FWHM change of BaM and substituted BaM showed 0.15 to 0.16 at 1200°C, and 0.21 to 0.29 at 900°C. This difference of FWHM could be explained by the crystallinity and crystal size of BaM

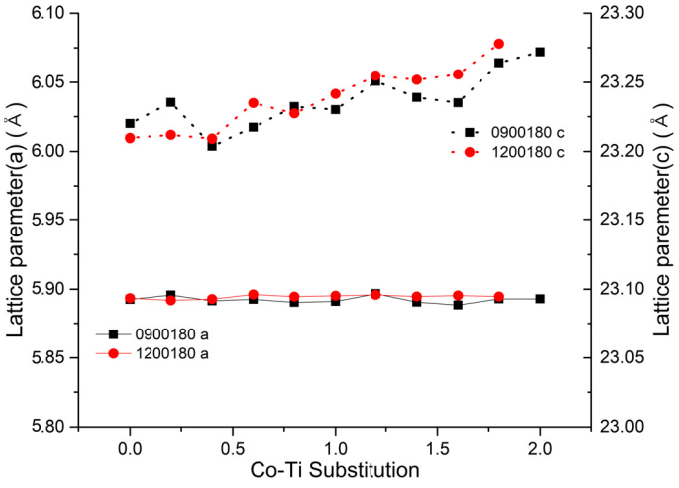

a) Lattice parameter

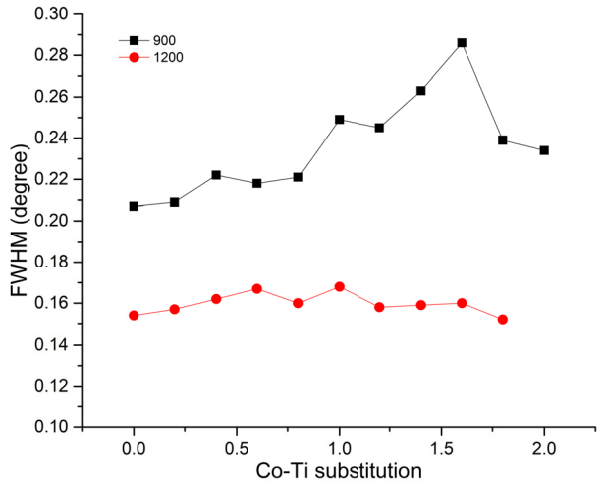

b) FWHM

Fig. 3. a) Lattice parameter and b) FWHM of BaM and substituted BaM with annealing temperature of 900°C and 1200°C

and substituted BaM. A low FWHM means sharp peak shape, high crystallinity, and large crystal size. Thus, it can be explained that the annealed powder at 1200°C revealed more crystallinity and large crystal size than the annealed powder at 900°C. And it could be confirmed with SEM images.

The SEM images of the annealed powders at 900°C and 1200°C are displayed in Fig. 4a) and b). The annealed powder at 1200°C revealed crystal size of 500 nm to 1μm, and the annealed powder at 900°C revealed the crystal size of 50 nm to 200 nm. The annealed powder of 1200°C showed 7.5 times larger crystal than the annealed powder at 900°C. This could be explained that the 1200°C annealing process provides sufficient energy for crystal growth, and it could be confirmed by the heat flow curve in Fig. 1.

B-H loops of the annealed samples at 900°C and 1200°C are displayed in Fig. 5. And the change of saturation magnetization and coercive force is displayed in Fig. 6. It could be seen that the saturation magnetization of the annealed BaM at 900°C and 1200°C were 54 emu/g and 57.5 emu/g, respectively. As seen in Fig. 6, the saturation magnetization was decreased to 22 emu/g and 9.5 emu/g with Co-Ti substitution ratio increasing to 2.0. This was because the substitution ions Co^{2+} and Ti^{4+} have net moments smaller than Fe^{3+} ions. The net moment of Fe^{3+} was $5\mu_b$, and Co^{2+} and Ti^{4+} were $3\mu_b$ and $0\mu_b$, respectively.

Also, looking at the B-H loop in Fig. 5, it could be seen that the annealed powder at 900°C exhibits soft magnetic properties at above the ratio of substitution ion of 1.0, and the annealed powder at 1200°C exhibits soft magnetic properties at above the ratio of substitution ion of 0.8. It could be confirmed that the hard magnetic property changed to the soft magnetic property with the increasing of the substitution ion ratio. It was confirmed that the substitution rates at which the changes occurred were 1.0 and 0.8, respectively, at 900°C and 1200°C. This difference was attributed to be due to the higher crystallinity of the annealed

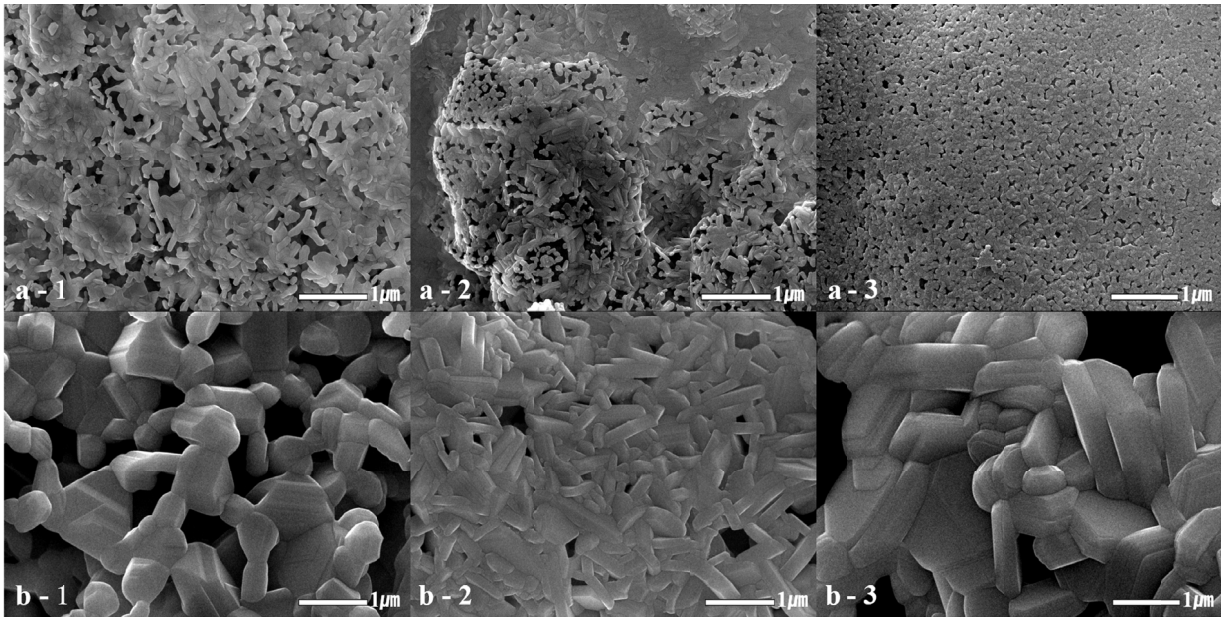

Fig. 4. SEM image of annealing temperature of a) 900°C and b) 1200°C (a-1: BaM, a-2: Ba Co1 Ti1 M, a-3: Ba Co2 Ti2 M, b-1: BaM b-2: Ba Co1 Ti1 M, and b-3: Ba Co2 Ti2 M)

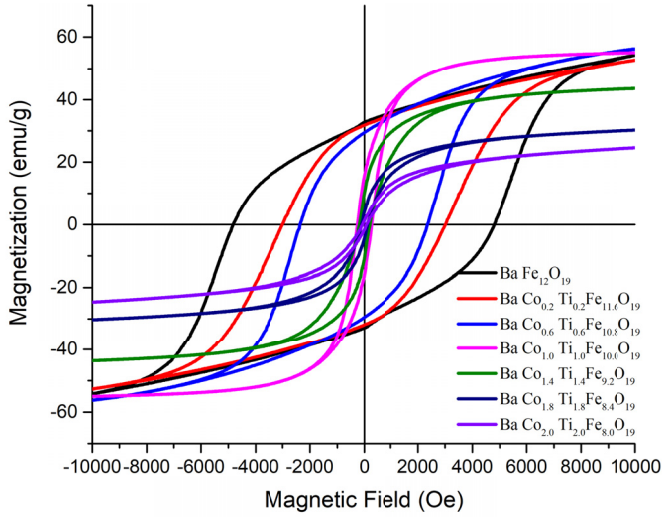

a) 900°C Anneling

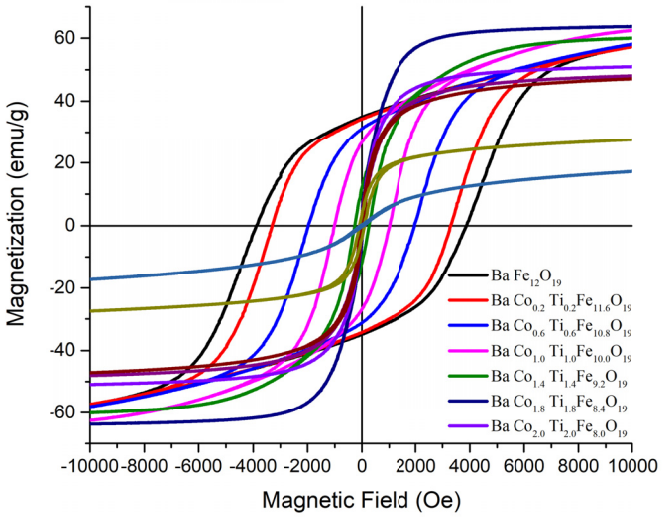

b)1200°C Anneling

Fig. 5. B-H curve of BaM and substituted BaM with annealing temperature of a) 900°C and b) 1200°C (±10,000 Oe)

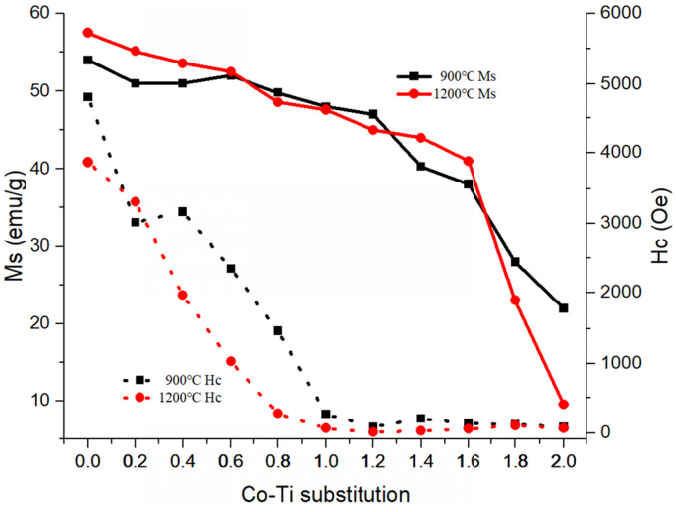

Fig. 6. Saturation magnetization (M_s) and Coercive force (H_c) of BaM and substituted BaM with annealing temperature at 900°C and 1200°C

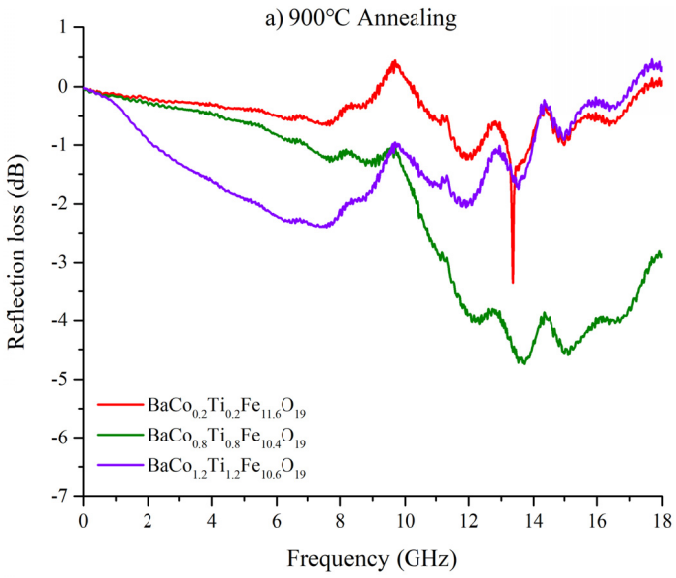

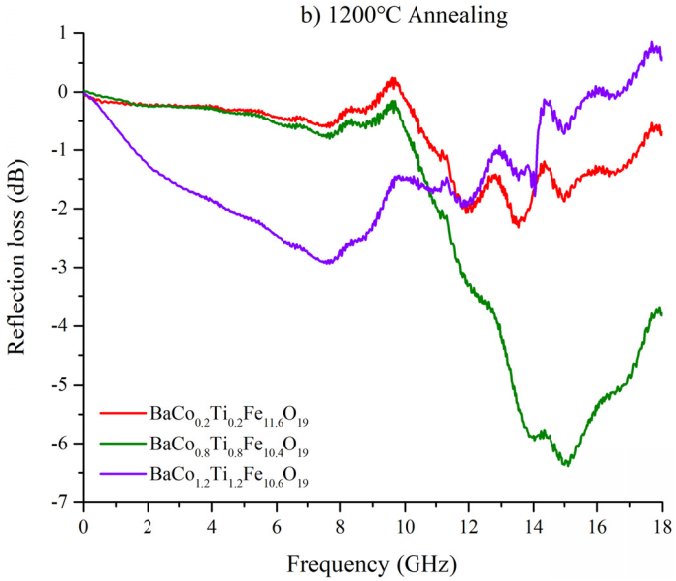

Fig. 7. Reflection loss of substituted BaM with annealing temperature at 900°C and 1200°C (thickness: 3 mm)

powder at 1200°C than the annealed powder at 900°C, which can be confirmed by the FWHM of the above mentioned XRD peak. The FWHM of 900°C and 1200°C were 0.29 and 0.15, respectively, thus, it can be confirmed that the annealed powder at 1200°C had larger crystal size than the annealed powder at 900°C. It was confirmed by the SEM images in Fig. 4. The annealed powder at 1200°C was confirmed that it has lower coercive force than 900°C annealing at the same substitution ratio, because of larger crystal size and more domain wall.

The hard magnetic property of the M-type ferrite was due to the easy magnetization axis fixed to the c-axis [2]. It could be explained indirectly by the coercive force change. In the Fig. 5 and Fig. 6, the coercive force was decreased 4,800 Oe and 3,870 Oe to 260 Oe and 269 Oe and the change of B-H loop shape was observed with the increase of the substitution ion ration to 2.0. Thus, it can be explained that the easy magnetization axis fixed to c-axis of BaM, which was weakened by the ratio of substitution ion of Co-Ti increasing to 2.0. Further, in the annealed samples

at 900°C of the ratio of substitution ion above 1.0 and the annealed samples at 1200°C of the ratio of substitution ion above 0.8 shown soft magnetic properties. Thus, it can be confirmed indirectly that the easy magnetization axis was changed from the c-axis to the a-b plane direction.

We have analyzed the wave absorption frequency change according to the change of easy magnetization axis of BaM. Reflection loss of the annealed powder at 900°C and 1200°C are displayed in Fig. 7. In case of the substitution ratio under the 0.8, the annealed powder at 900°C and 1200°C showed the wave absorption range above 10 GHz. In case of substitution ratio 0.8, the annealed powder at 900°C revealed wave absorption at 12.2, 13.6, and 15.1 GHz. And the annealed powder at 1200°C revealed wave absorption at 14, 14.9, and 16.9 GHz. On the contrary, In case of the substitution ratio of 1.0 to 1.6, the annealed powders at 900°C and 1200°C had the wave absorption range less than 10 GHz. It was confirmed that the wave absorption range changed when the substitution ratio changed.

As mentioned above, it was explained that the magnetic properties of BaM were changed by substitution ion, and the substitution ion ratio increasing to 1.0 and 0.8 caused easy magnetization axis change from c-axis to a-b plane. The change of easy magnetization axis was confirmed that the coercive force was decreased 4,800 and 3,870 Oe to 260 and 269 Oe, respectively.

4. Conclusions

In this study, $BaFe_{12-2x}Co_xTi_xO_{19}$ (X : 0 to 2.0, 0.2) powders were synthesized by sol-gel process. TG-DTA, XRD, SEM, VSM, and Network analyzer were measured in order to influence easy magnetization axis change on the wave absorption frequency range change. The hard magnetic properties of BaM are attributed to the easy axis of magnetization, which is strongly fixed to the c-axis. Co and Ti ions were substituted to $4f_1$ and 2b sites in the c-axis direction for change the easy magnetization axis to the a-b plane direction. As a result, in the case of the annealed powder at 900°C and 1200°C of substitution ratio of 0.8 and 1.0, respectively, it was confirmed that the coercive force decreased 4,800 and 3,870 Oe to 260 and 269 Oe, respectively. Based on this, it could confirm the change of easy magnetization axis. And it could confirm that the change of the easy magnetization axis affected the change of the wave absorption range. It was confirmed that the wave absorption range of beyond 10 GHz was observed before the easy magnetization axis change and the wave absorption range was observed less than 10 GHz range after the easy magnetization axis changed to a-b plan direction. It was confirmed that $BaFe_{12-2x}Co_xTi_xO_{19}$(x = 0.8 to 1.6) was synthesized by the sol-gel process can be used as a wave absorber in the X-band region of 10 GHz less.

REFERENCES

[1] L.S.I. Liyanage, S. Kim, Y. Hong, J. Park, S.C. Erwin, Cond-mat. Mtrl-sci, 1209.5143v2 (2013).

[2] M. Mohebbi, K. Ebnabbasi, C. Vittoria, IEEE. T. Magn. **49**, 4207-4209 (2013).

[3] K. Okayama et al., J. Magn. Soc. Japan, **22**, 297(1998).

[4] T. Kagotan, D. Fujiwara, J. Mag. Mag. Mat. 272-276 (2004).

[5] S. Kanagesan, S. Jesurani, R. Velmurugan, T. Kalaivani, J. Mater. Sci-Mater. El. **23**, 952-925 (2012).